Advances in Science and Technology Research Journal

Advances in Science and Technology Research Journal, 2026, 20(7), 454–469
https://doi.org/10.12913/22998624/219654
ISSN 2299-8624, License CC-BY 4.0

Received: 2026.02.21
Accepted: 2026.05.15
Published: 2026.06.01

Nonlinear model predictive control with online estimation of the specific growth rate in bioethanol fermentation

Piotr Skupin[1]

[1] Department of Automatic Control and Robotics, Silesian University of Technology, ul. Akademicka 16, 44-100 Gliwice, Poland
* E-mail: piotr.skupin@polsl.pl

ABSTRACT

The paper addresses the problem of stabilization of a continuous fermentation process for efficient production of the bioethanol. The mathematical model of the process is derived on the assumption that the inhibitory effect of ethanol concentration is delayed in time and including decay of microorganism cells. Stability analysis of the open-loop system demonstrates unstable behavior of the fermentation process in a range of dilution rates. The effect of kinetic parameters on the dynamical behavior of the process and steady-state ethanol concentrations is also studied. To stabilize the fermentation process a nonlinear model predictive control (NMPC) technique is applied. To deal with plant–model mismatch, an observer that estimates the microbial specific growth rate is designed. The effectiveness of the proposed NMPC-based strategy is evaluated under model uncertainty and measurement noise, and compared with two alternative NMPC-based strategies.

Keywords: nonlinear model predictive control, fermentation process, parameter estimation, parameter uncertainty.

INTRODUCTION

Bioethanol is simply ethanol that can be made from organic wastes containing sugars. As traditional fossil fuels are about to deplete, there is a growing interest in efficient production of the bioethanol [1]. To improve efficiency of the fermentation process continuous reactors are preferred. They do not require additional processing time for emptying, cleaning, or filling up the reactor vessel as in the case of batch processes. Moreover, continuous reactors are more flexible in control [2]. However, in the case of continuous ethanol fermentation processes, it is not unusual to observe self-sustained oscillations in key process variables at constant inlet conditions [3]. It is believed that oscillatory behavior results from delayed response of microorganisms to high ethanol concentrations and this hypothesis was studied experimentally in [3,4] and theoretically in [5,6].

The oscillatory mode of operation is often avoided in practice because it may lead to lower average ethanol concentrations and increased energy expenditure in downstream distillation processes [4,7,8]. Different approaches aiming to eliminate the oscillations can be classified into open-loop and closed-loop control strategies. Examples of the open-loop strategies include the use of selective membranes [9], cascade of reactors [10], additional substrates [11], and manipulation of the flow rate of substrate or its inlet concentration [12–16]. However, in the presence of plant-model mismatch or external disturbances, the open-loop strategies may be inefficient. In that case one can apply closed-loop strategies that constantly adjust their control actions based on the measured process variables. Among the various closed-loop control techniques, the most common control algorithm is the classical proportional-integral (PI) controller. When the manipulated variable is properly chosen and the PI controller is properly tuned, it can be very effective in stabilizing nonlinear processes [17,18]. However, when the process parameters are not known exactly (parameter uncertainty), the PI controller

must be tuned more conservatively, which may affect control performance [19].

An alternative to classical PI controllers is the use of advanced control techniques such as model predictive control (MPC). In MPCs algorithms, control actions are computed based on the minimization of an objective function subject to constrains. As a result, these algorithms can be very effective in control of fermentation processes [20,21]. However, in the presence of plant-model mismatch, MPC algorithms often produce a nonzero offset and the inaccurate models used for prediction may degrade control performance. To deal with plant-model mismatch in the control of fermentation processes, an offset-free nonlinear MCP (NMPC) was proposed in [22] and studied for the fermentation process in [23]. The offset-free NMPC ensured very good setpoint tracking without offset, but the controller was tested assuming no structural differences between the model and the process. Another approach is to use neural-network models to describe the relationships between the process inputs and outputs. While the application of neural-network models for nonlinear systems is very common, they may require large amounts of measurement data to achieve accurate predictions. Thus, a recent study by Bannoud et al. [24] proposes a mixed model predictive control (MMPC) approach to find balance between robustness and computational efficiency in neural-network-based MPCs. In turn, a robust MPC with integral action proposed in [25], outperformed neural-network-based MPC.

To improve the accuracy of fermentation models used for prediction and to ensure zero offset, parameter observers can be employed to estimate unknown model parameters [26]. However, the number of unknown parameters that can be estimated usually depends on the available measurement data. Another issue is how the observer dynamics influence control performance. Therefore, in this paper an alternative approach is presented, in which the NMPC is based on a parameter observer that estimates only one of the unknown kinetic parameters. The effectiveness of the proposed controller is studied in the presence of parameter uncertainty, differences in process-model structure, and measurement noise. The rest of the paper is organized as follows. The next section gives details on the mathematical model of the fermentation process and stability analysis of the open-loop system is caried out. Section 3 describes the NMPC design and Section 4 presents closed-loop simulation results. Finally, Section 5 concludes the paper.

MATHEMATICAL MODEL AND STABILITY ANALYSIS OF THE OPEN-LOOP FERMENTATION PROCESS

Mathematical model of the continuous ethanol fermentation process is derived using the following assumptions [6]: the reactor content is well-mixed, the growth of microorganisms is limited by a single substrate and inhibited by high ethanol concentrations, but the inhibitory effect is delayed in time. Moreover, the model includes the decay of microorganisms cells. Thus, equations for the open-loop system are as follows:

$$\frac{dS}{dt} = D(S_{in} - S) - \frac{\mu(S, P_\tau)}{Y_{xs}} X \tag{1}$$

$$\frac{dX}{dt} = -DX + \mu(S, P_\tau)X - k_d X \tag{2}$$

$$\frac{dP}{dt} = -DP + \mu(S, P_\tau)Y_p X \tag{3}$$

$$\mu(S, P_\tau) = \frac{\mu_m S}{S + K_s} \cdot \frac{K_i}{P_\tau + K_i} \tag{4}$$

where: S_{in}, S are the inlet and outlet substrate concentrations; X is the microorganisms concentration; P is the product (ethanol) concentration; $P_\tau := P(t-\tau)$ is the delayed product concentration and τ is the delay time; D is the dilution rate; Y_{xs} is the biomass yield coefficient (the amount of biomass produced per one gram of the substrate consumed); Y_p is the product yield coefficient (the amount of product formed per one gram of the biomass); k_d is the microorganisms death rate; $\mu(S,P_\tau)$ is the specific growth rate; μ_m is the maximum specific growth rate; K_s is the half-saturation constant; K_i is the inhibitory constant.

The mathematical model (1–4) with k_d=0 was verified against the experimental data in [6] and numerical values of its parameters are shown in Table 1. In this study, a nonzero microorganism death rate k_d>0 is added to the model (1–4).

First, the fermentation system given by (1–4) is analyzed in the open-loop configuration.

Table 1. Model parameter values

Parameter	S_{in}	μ_m	K_s	K_i	Y_{xs}	Y_p	τ	k_d
Value	50 g/L	0.78 1/h	1.73 g/L	3.89 g/L	0.0486 g/g	9.098 g/g	23.0 h	0.02 1/h

The system (1–4) has two equilibrium points: $E_1 = (S_1^*, X_1^*, P_1^*) = (S_{in}, 0, 0)$ when the microorganisms are washed out of the reactor vessel and the nonzero equilibrium $E_2 = (S_2^*, X_2^*, P_2^*)$, where $S_2^*, X_2^*, P_2^* > 0$. The nonzero equilibrium can be found from the following equations:

$$\mu(S_2^*, P_2^*) = k_d + D \tag{5}$$

$$DP_2^* = (k_d + D) Y_p X_2^* \tag{6}$$

$$P_2^* = (S_{in} - S_2^*) Y_{xs} Y_p \tag{7}$$

Local stability conditions for the open-loop fermentation system can be determined by linearizing the system Equations 1–4 at each of the equilibrium points assuming that the dilution rate D and inlet substrate concentration S_{in} are constant parameters:

$$\frac{ds}{dt} = -\left(D + \frac{X_i^*}{Y_{xs}} \cdot \frac{\partial \mu^*}{\partial S}\right) s - \frac{\mu^*}{Y_{xs}} x - \frac{X_i^*}{Y_{xs}} \cdot \frac{\partial \mu^*}{\partial P_\tau} p_\tau \tag{8}$$

$$\frac{dx}{dt} = X_i^* \frac{\partial \mu^*}{\partial S} s - (D + k_d - \mu^*) x + X_i^* \frac{\partial \mu^*}{\partial P_\tau} p_\tau \tag{9}$$

$$\frac{dp}{dt} = Y_p X_i^* \frac{\partial \mu^*}{\partial S} s + \mu^* Y_p x - Dp + Y_p X_i^* \frac{\partial \mu^*}{\partial P_\tau} p_\tau \tag{10}$$

where: s, x, p, p_τ are state variables in the linearized system and asterisk symbols indicate calculations at the equilibrium point E_i (i=1,2).

The characteristic equation at the i-th equilibrium point E_i (i=1,2) has the following form:

$$\det(I_3 \lambda - J_0 - J_1 e^{-\lambda \tau}) = 0 \tag{11}$$

where: I_3 is a 3 × 3 identity matrix, and J_0 and J_1 are 3 × 3 matrices with coefficients of the linearized system (8–10).

Thus, the characteristic equation at the washout equilibrium point $E_1 = (S_{in}, 0, 0)$:

$$(\lambda + D)^2 (\lambda + D + k_d - \mu(S_{in}, 0)) = 0 \tag{12}$$

and at the nonzero equilibrium point $E_2 = (S_2^*, X_2^*, P_2^*)$:

$$\Phi(\lambda) + \Psi(\lambda) e^{-\lambda \tau} = 0 \tag{13}$$

where:

$$\Phi(\lambda) = (\lambda + D)\left(\lambda^2 + \left(D + \frac{X_2^*}{Y_{xs}} \cdot \frac{\partial \mu^*}{\partial S}\right)\lambda + \frac{X_2^*}{Y_{xs}} \cdot \frac{\partial \mu^*}{\partial S}(D + k_d)\right) \tag{14}$$

$$\Psi(\lambda) = -Y_p X_2^* \frac{\partial \mu^*}{\partial P_\tau} (\lambda + D)(\lambda + D + k_d) \tag{15}$$

Since D>0, the washout equilibrium $E_1 = (S_{in}, 0, 0)$ is locally asymptotically stable when D>D_c and D_c=$\mu(S_{in},0)$−k_d is a critical dilution rate. It means that the microorganisms are washout of the reactor vessel when the dilution rate D is too high. Thus, the dilution rate D must be kept below its critical value D_c.

Regarding the nonzero equilibrium $E_2 = (S_2^*, X_2^*, P_2^*)$ the stability conditions not only depend on the dilution rate D, but also on the delay time τ. Since λ=−D is one of the roots of (13), further analysis is carried out for the reduced order equation:

$$\lambda^2 + (D + a)\lambda + a(D + k_d) + b(\lambda + D + k_d) e^{-\lambda \tau} = 0 \tag{16}$$

where: $a = \frac{X_2^*}{Y_{xs}} \cdot \frac{\partial i^*}{\partial S}$, $b = -Y_p X_2^* \frac{\partial i^*}{\partial P_\tau}$. Please note that all the coefficients in (16) are positive numbers as $X_2^* > 0$, $\frac{\partial i^*}{\partial S} > 0$, $-\frac{\partial i^*}{\partial P_\tau} > 0$, and the distribution of roots of (16) can be studied using the following lemma by Ruan and Wei [27].

Lemma [27]: Let W be a quasi-polynomial and $\tau_i \geq 0$ (i=1,2,...,m) are constant delay times:

$$W(\lambda,\tau_1,\tau_2,....,\tau_m)=\lambda^n+p_1^{(0)}\lambda^{n-1}+....+$$
$$+p_{n-1}^{(0)}\lambda+p_n^{(0)}+\left(p_1^{(1)}\lambda^{n-1}+....+p_{n-1}^{(1)}\lambda+p_n^{(1)}\right)e^{-\lambda\tau_1}+$$
$$+...+\left(p_1^{(m)}\lambda^{n-1}+....+p_{n-1}^{(m)}\lambda+p_n^{(m)}\right)e^{-\lambda\tau_m}=0$$

where: $p_j^{(i)}$ (i=0,1,...,m; j=1,2,...,n) are real numbers. Then, as (τ_1,τ_2,...,τ_m) varies, the sum of the multiplicities of zeros of W on the open right half-plane can change only if a zero appears on or crosses the imaginary axis.

First, the stability analysis is caried out for τ=0, then (16) is rewritten to:

$$\lambda^2+(D+a+b)\lambda+ \\ +(a+b)(D+k_d)=0 \tag{17}$$

and the open-loop fermentation process (1) is locally asymptotically stable at $E_2=(S_2^*,X_2^*,P_2^*)$ for any positive X_2^* >0 that can be achieved for 0<D<D_c.

If τ>0, then the open-loop fermentation process (1–4) can only be destabilized, if there exists a pair of complex roots of (16) that crosses the imaginary axis. Thus, substituting $\lambda=i\omega$ (ω>0) into the equation (16) and separating real and imaginary parts one can obtain:

$$b(D+k_d)\cos(\omega\tau)+ \\ +\omega b\sin(\omega\tau)=\omega^2-a(D+k_d) \tag{18}$$

$$\omega b\cos(\omega\tau)-b(D+k_d)\sin(\omega\tau)= \\ =\omega(D+a) \tag{19}$$

and then:

$$\cos(\omega\tau)=\frac{a(D+k_d)^2-\omega^2(2D+a+k_d)}{\omega^2 b+(D+k_d)^2 b} \tag{20}$$

$$\sin(\omega\tau)=-\frac{\omega^2+\omega(D+k_d)}{\omega^2 b+(D+k_d)^2 b}(D+a) \tag{21}$$

Then, from the Pythagorean trigonometric identity one can obtain the equation for z:=ω^2>0:

$$z^2+z(D^2-2ak_d+a^2-b^2)+ \\ +(a^2-b^2)(D+k_d)^2=0 \tag{22}$$

The Equation 22 has two positive roots if the following conditions are satisfied:

$$\Delta\geq 0 \tag{23}$$

$$D^2-2ak_d+a^2-b^2<0 \tag{24}$$

$$(a^2-b^2)(D+k_d)^2\geq 0 \tag{25}$$

or one positive root if the following condition is satisfied:

$$(a^2-b^2)(D+k_d)^2<0 \tag{26}$$

where: Δ is the discriminant of Equation 22.

Since the open-loop fermentation system is asymptotically stable for τ=0, the equilibrium point $E_2=(S_2^*,X_2^*,P_2^*)$ may become unstable for a sufficiently long delay time τ. If the conditions (23–25) are satisfied, then there exist two positive roots z_1 and z_2 with the corresponding ω_1 and ω_2, and the corresponding delay times can be found from (20–21):

$$\tau_k=\frac{1}{\omega_k}arccos\left(\frac{a(D+k_d)^2-\omega^2(2D+a+k_d)}{\omega^2 b+(D+k_d)^2 b}\right)+ \\ +\frac{2n\pi}{\omega_k} \tag{27}$$

where: k=1,2, n=0,±1,±2,…

In the same way, the corresponding delay time can be obtained when the Equation 22 has only one positive root. Now, the crossing direction of a pair of purely imaginary roots $\lambda_k=\pm i\omega_k$ as τ increases can be determined from the following condition:

$$sign\left\{Re\left(\frac{d\lambda}{d\tau}\Big|_{\lambda=i\omega_k}\right)\right\}= \\ =sign\left\{\begin{matrix}\omega_k^4+(D+k_d)^2\\(2\omega_k^2+D^2-2ak_d)\\(\omega_k^2(D+a)^2+(a(D+k_d)-\omega_k^2)^2)\\(\omega_k^2+(D+k_d)^2)\end{matrix}\right\}= \\ =sign\{\omega_k^4+(D+k_d)^2(2\omega_k^2+D^2-2ak_d)\} \tag{28}$$

If the sign of (28) is positive, then a pair of purely imaginary roots $\lambda_k=\pm i\omega_k$ crosses the imaginary axis from the left to the right half-plane as the delay time τ increases and the open-loop fermentation process becomes unstable. As a result, one can also observe self-sustained oscillations of the ethanol concentration.

Figure 1 (left plot) shows steady-state ethanol concentrations for the nominal parameter values given in Table 1. The continuous lines represent stable behavior, while the dotted lines represent unstable behavior. For dilution rates between 0.1426 and 0.6444 1/h, the fermentation process

is unstable and self-sustained oscillations of the ethanol concentration can be observed. This is clearly shown in Figure 1 (right plot), when the dilution rate is changed from 0.1 to 0.15 1/h in the open-loop system.

By using (23)–(27), the effect of different kinetic parameters on steady-state ethanol concentrations and dynamical behavior of the fermentation process can be studied. Figure 2 shows steady-state diagrams for two kinetic parameters (the maximum specific growth rate μ_m and the inhibitory coefficient K_i) that have the most significant effect on the dynamical behavior of the process. The diagrams are obtained for nominal parameter values (Table 1) and kinetic parameters that are increased or decreased by 30%. As it is clearly seen, the range of dilution rates with unstable behavior strongly depends on the kinetic parameters. Thus, in order to stabilize the fermentation process, a closed-loop control strategy is required. Note that not only can the dynamical behavior change depending on the dilution rate D, but the process gain can also change (Figures 1 and 2), which poses an extra challenge for a controller.

PREDICTIVE CONTROLLER DESIGN

The control goal is to stabilize the fermentation process in a wide range of operating conditions. The manipulated variable is the dilution rate D and the process variable is the ethanol concentration P. In this work an adaptive NMPC algorithm is proposed to stabilize the process and its effectiveness is compared with the classical and the offset-free NMCPs designed according to [22].

The predictive controllers are designed using the model (1–4) and based on the following assumptions:

- the microorganism death rate is set to zero $k_d=0$
- the only measured variable is the ethanol concentration $P(t)$
- only nominal values of kinetic parameters (μ_m, K_s, K_i) and the inlet substrate concentration S_{in} are known and their true values can differ up to ±30% (parameter uncertainty). The nominal parameters are used for designing predictive controllers.

The assumption (i) is often made as the death rate of microorganism cells is usually not known in practice, but has smaller value compared to the applied dilution rate D. According to (ii), the ethanol concentration can be measured online, but the measurements can be corrupted by noise [28,29]. The other state variables (substrate and microorganism concentrations) are estimated by using an observer. As the adaptive NMPC is designed for the nominal parameter values given in Table 1 (assumption (iii)), the control algorithm is implemented with an extra parameter observer to ensure zero offset. Thus, the adaptive NMPC can be presented as follows:

$$\min_{u_n} Q\sum_{n=1}^{Np}(P_{sp}-P)^2 + R\sum_{n=0}^{Nc-2}\Delta u_n^2 \qquad (29)$$

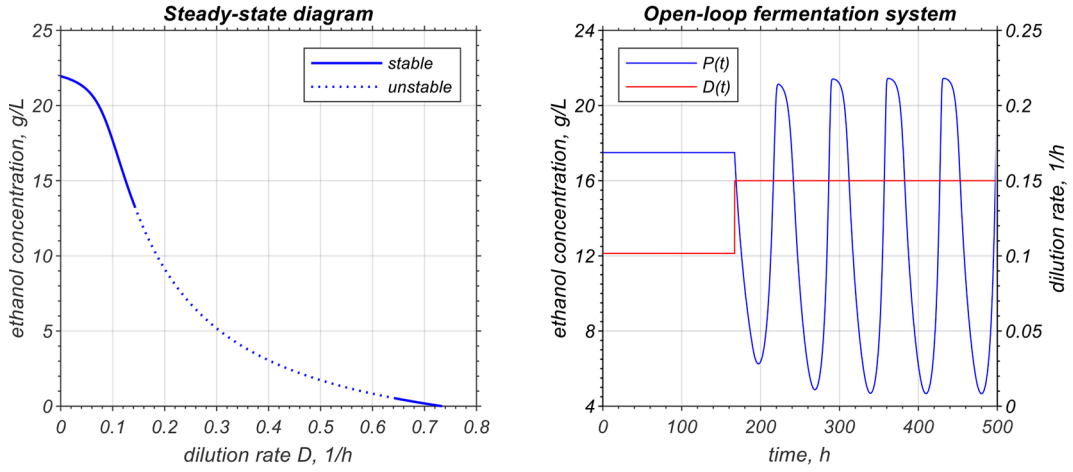

Figure 1. Dynamical behavior of the open-loop fermentation system. The left plot: the steady-state ethanol concentration P versus dilution rate D. The right plot: the response of the fermentation process to a step change in the dilution rate $D(t)$

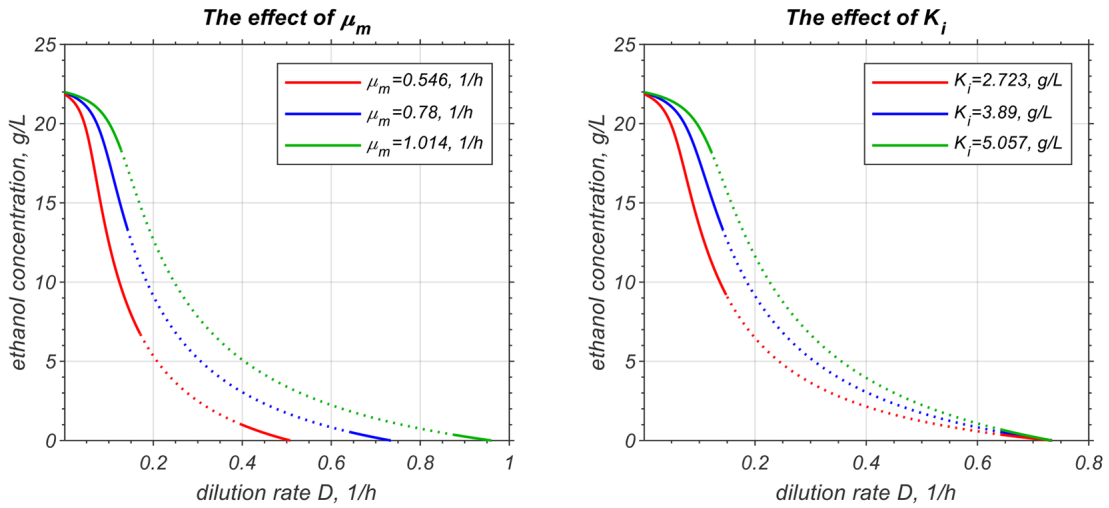

Figure 2. The effect of kinetic parameters on steady-state ethanol concentration and dynamical behavior of the open-loop fermentation system. Stable and unstable behavior is represented by continuous and dotted lines, respectively

subject to:

$$x_{n+1} = \varphi(x_{n+1}, x_n, u_n, \hat{p}),\ n=0,1,\ldots,N_p-1 \quad (30)$$

$$x_0 = x(0) \quad (31)$$

$$u^{\min} \le u_n \le u^{\max},\ n=0,1,\ldots,N_p-1 \quad (32)$$

where: N_p, N_c are prediction and control horizons, respectively; Q, R are weighting coefficients.

The first term in (29) is for driving the fermentation system to the setpoint product concentration P_{sp}. The last term is usually added to suppress too large increments in the control signal computed by the NMPC. The equality constraints in (30) are discretized state-space Equations 1–4 using implicit Euler method with $x_n=[S_n\ X_n\ P_n]^T$. To ensure zero offset, the discretized state-space Equation 30 contain the estimated parameter $\hat{p}$. The equality constraints (31) result from initial conditions that change at each sampling time instant (initialization of the optimization problem). Finally, the last inequality constraints (32) are typical constraints on the manipulated variable (dilution rate D). For the fermentation system, it is required that D is always positive (continuous flow reactor) and, as shown in the stability analysis of the open-loop system, D should be smaller than the critical dilution rate $D_c=\mu(S_{in},0)$. Hence, $D^{\min}\le D(t)\le D^{\max}<D_c$.

Estimation of unmeasured state variables

Due to specific structure of the model Equations 1–4 and assuming zero death rate ($k_d=0$), the unmeasured substrate $S(t)$ and microorganism $X(t)$ concentrations can be estimated using the asymptotic observer [30] and measured ethanol concentrations:

$$\frac{d\hat{Z}_1}{dt} = D(S_{in}Y_{xs} - \hat{Z}_1) \quad (33)$$

$$\frac{d\hat{Z}_2}{dt} = -D\hat{Z}_2 \quad (34)$$

$$\hat{S} = \frac{Y_p\hat{Z}_1 + \hat{Z}_2 - P}{Y_{xs}Y_p} \quad (35)$$

$$\hat{X} = \frac{P - \hat{Z}_2}{Y_p} \quad (36)$$

where: $\hat{Z}_1$ and $\hat{Z}_2$ are observer state variables; $\hat{S}$ and $\hat{X}$ are estimated substrate and microorganism concentrations, respectively.

Please note that according to (34), $\hat{Z}_2$ tends to 0 with the rate specified by the dilution rate $D>0$, irrespective of the changes in other process parameters (e.g., changes in the inlet concentration S_{in}). When $\hat{Z}_2$ is very close to zero, the microorganism concentration X can be directly estimated from (36) based only on the measured ethanol concentration P. The convergence rate of $\hat{Z}_1$ also depends on

the dilution rate D. Thus, there are not any tuning parameters. Cell decay (k_d>0) can also be included in the asymptotic observer design, but as previously mentioned, the exact value of k_d is not always known in practical applications. Assuming k_d=0 in the observer Equations 33–36 does not affect its stability, but this will introduce estimation errors in the estimate $\hat{X}$. It should also be noted that uncertainty in the inlet substrate concentration S_{in} also contributes to estimation errors in the estimate $\hat{S}$, but does not affect the stability of the observer (33–36).

Estimation of specific growth rate

Although the specific growth rate $\mu(S,P_\tau)$ in (1–4) is a function of substrate and delayed ethanol concentrations, it is treated as a time-varying model parameter $\mu(t)$ and estimated using a parameter observer. Treating $\mu(S,P_\tau)$ as one of the model parameters greatly simplifies the observer design, since there is no need to specify the structure for $\mu(t)$. Therefore this approach was previously applied in various bioreactor systems [31–34]. The parameter observer is designed according to [30, 31] and, regarding the parameter $\mu(t)$, one of the design assumptions is that the time derivative of $\mu(t)$ is bounded. Assuming no cell decay (k_d=0) the observer equations are as follows:

$$\frac{d\hat{P}}{dt} = -DP + Y_p\hat{\mu}\hat{X} + \Omega(P-\hat{P}) \tag{37}$$

$$\frac{d\hat{\mu}}{dt} = \Gamma(P-\hat{P}) \tag{38}$$

$$\hat{\mu} = \hat{\mu}_m \frac{\hat{S}}{\hat{S}+K_s}\cdot\frac{K_i}{K_i+P_\tau} \tag{39}$$

where: Ω and Γ are the observer parameters to be tuned.

As soon as the new estimate μ is available, the maximum specific growth rate μ_m in the model (1–4) is updated using the Equation 39 and the corrected model (1–4) with k_d=0 is used by the adaptive NMPC algorithm (29–32). As explained earlier, when $\hat{Z}_2$ is very close to zero, the estimated microorganism concentration $\hat{X}$ is very close to P/Y_p and this does not change as long as $D(t)$>0, which is ensured by the predictive controller. It should be noted that the estimate $\hat{X}$ is not exactly equal to its true value X when $\hat{Z}_2 \approx 0$ in (34), which results form nonzero death rate (k_d>0) in the real process (1–4). However, at steady-state conditions the true concentration X can be obtained from $\hat{X}$ by multiplying it by $D/(D+k_d)$ provided that k_d is known. Hence, by using the observer (37–39) with $\hat{X}\neq X$, the estimated specific growth rate parameter μ will differ from its true value μ, because the estimation error in $\hat{X}$ is compensated by μ.

Then, the observer parameters Ω and Γ are chosen by studying the error dynamics for (37–39) and assuming no cell decay (k_d=0). In that case, $\hat{X}$ in (37) can be replaced with its true value X:

$$\frac{de_1}{dt} = -\Omega e_1 + Y_p X e_2 \tag{40}$$

$$\frac{de_2}{dt} = -\Gamma e_1 + \frac{d\mu}{dt} \tag{41}$$

where: $e_1 = P-\hat{P}$ and $e_2 = \mu-\hat{\mu}$.

The eigenvalues of (40–41) can be easily determined by analyzing the characteristic equation of (40–41) and the parameters Ω and Γ can be chosen by placing both poles of the observer (40–41) at $\lambda_1=\lambda_2=\omega_0$. Hence, the observer parameters are: $\Omega = 2\omega_0$ and $\Gamma = \omega_0^2/(Y_pX)$, where ω_0 is the only tuning parameter and provided that X>0. Although the observer (40–41) is designed assuming no cell decay (k_d=0), it will be shown in simulation experiments that the estimate μ ensures zero offset in the adaptive NMPC and the observer is stable with $\Gamma = \omega_0^2/(Y_p\hat{X})$ where $\hat{X}\neq X$ and $\hat{X}$>0.

Finally, the structure of the proposed adaptive NMPC including the asymptotic and parameter observers is shown in Figure 3.

Classical and offset-free NMPCs

As mentioned earlier, the adaptive NMPC (29–32) is compared with the classical and offset-free NMPCs. The offset-free NMPC is designed as follows [22,35]:

$$\min_{u_n} Q\sum_{n=1}^{Np}(P_{sp}-P)^2 + R\sum_{n=0}^{Nc-2}\Delta u_n^2 \tag{42}$$

subject to:

$$x_{n+1} = \varphi(x_{n+1},x_n,u_n)+v,\ n=0,1,\ldots,N_p-1 \tag{43}$$

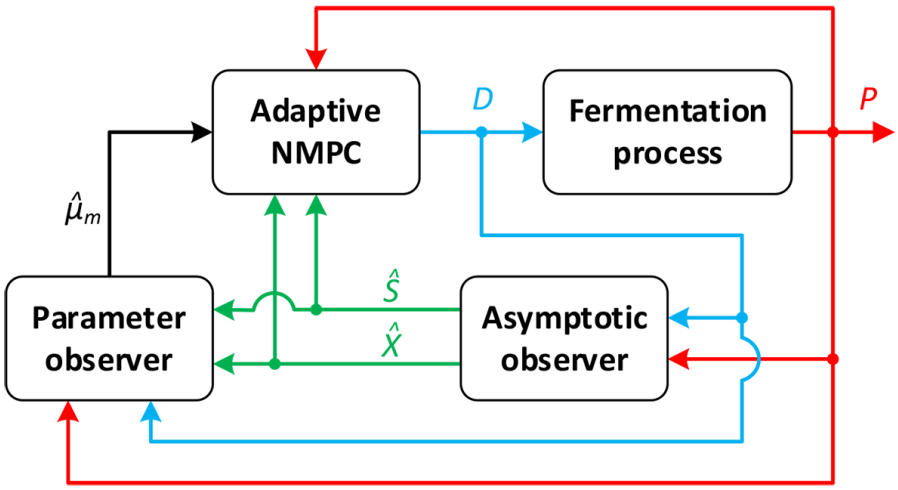

Figure 3. The control framework with the adaptive NMPC

$$x_0 = x(0) \tag{44}$$

$$u^{\min} \le u_n \le u^{\max},\ n=0,1,\ldots,N_p-1 \tag{45}$$

Compared to the adaptive NMPC (29–32), the offset-free NMPC is designed for nominal parameter values (Table 1) with k_d=0 and without the parameter observer (29–32). The state-space equations are also discretized using the implicit Euler method and the unmeasured substrate and microorganism concentrations are estimated using the asymptotic observer (33–36). The zero offset property is achieved by adding a constant correction term v to each of the state equations in (43), which is based on the measured state, previously estimated state variables, and previously applied manipulated variable: $v = x_0 - \varphi(x_0, x_{-1}, u_{-1})$.

In turn, the classical NMPC is designed according to (42–45), but assuming v=0 in (43), which means that no model correction is made.

Irrespective of the NMPC algorithm used, the optimization problem (29–32) or (42–45) is solved at each sampling time instant T_s in Matlab using IPOPT solver [36] and 2-core Intel i3-4150 CPU (3.5 GHz) with 12GB RAM. The simulation results are presented in the next section.

CLOSED-LOOP SIMULATION RESULTS

As mentioned earlier, the NMPCs are designed with k_d=0, while in the simulated fermentation process (1–4), a fraction of the microbial population undergoes decay at a rate given by k_d>0. Thus, including cell decay in the simulated "real" fermentation process allows testing the control performance in the presence of structural differences between the real process and its mathematical model. Hence, the predictive controllers are studied under differences in the model structure and taking into account three different scenarios.

- Scenario 1: all model parameters apart from S_{in} in the model Equations 1–4 are perfectly known only the inlet substrate concentration S_{in} is not know precisely and may differ up to 30% with respect to its nominal value of 50 g/L.
- Scenario 2: true kinetic parameters may differ up to 30% with respect to their nominal values, but are constant. The inlet concentration S_{in} is also not known precisely.
- Scenario 3: true kinetic parameters may vary over time and differ up to 30% with respect to their nominal values. The inlet concentration S_{in} is also not known precisely and the measured ethanol concentrations are corrupted by noise.

In each scenario, the same controller parameters and the same initial conditions for the observers are used. The controller sampling time is T_s=0.5 h, and the prediction and control horizons are set to N_p=100, N_c=50. The preliminary results show that the prediction horizon should be sufficiently long to capture both the effect of delayed ethanol concentration (τ=23 h) and the response that follows this delayed ethanol effect. No significant improvement was observed for longer prediction horizons. Although, no rigorous stability analysis is provided in the paper, in many practical cases, increasing the length of the prediction horizon promotes the stability of the closed-loop

system. Also, adding some terminal constraints to the optimization problem may help to ensure the stability of the closed-loop system [37]. In the presented case, the assumed length of the prediction horizon (N_p=100) ensured stable behavior of the closed-loop system. The weighting coefficients in the NMPC's objective functions are set to Q=1.0, R=0.5, and the only tuning parameter in the parameter observer (37–39) is set to ω_0=5.0 1/h. To avoid washout conditions in each scenario, the lower and upper constraints for dilution rate are set to $u^{min}=D^{min}$=0.01 1/h, $u^{max}=D^{max}$=0.5 1/h. The effectiveness of each control algorithm is additionally evaluated by computing the integral of squared error (*ISE*) indicator:

$$ISE = \int_0^{t_f} (P_{sp} - P(t))^2 dt \tag{46}$$

Scenario 1

In the first scenario, effectiveness of the NMPC is studied under the assumption that all model parameters apart from S_{in} in the system Equations 1–4 are perfectly known. Only the nominal value of S_{in}=50 g/L is known and used by the NMPC, but the true inlet substrate concentration may vary depending on the sugar content in various organic wastes used in bioethanol production. Hence, it is assumed that the true inlet substrate concentration S_{in} varies in a step-wise manner between 40 and 60 g/L.

As shown in Figure 4, both the adaptive and offset-free NMPCs can perfectly track the setpoint ethanol concentration P_{sp}. The zero offset can be achieved even for step changes in the unmeasured inlet substrate concentration S_{in} and the computed *ISE* indicators are: $ISE_{adapt.}$=1579.6 (adaptive NMPC) and $ISE_{of.}$=1580.6 (offset-free NMPC). In the case of the classical NMPC, it is not a surprise to observe a nonzero offset that results from the plant-model mismatch and the resulting performance indicator is $ISE_{class.}$=1639.1. Regarding the oscillatory behavior that was observed in the open-loop system, each NMPC controller is able to stabilize the fermentation process and eliminate the oscillations (Figure 4).

The corresponding time courses of the estimated substrate $\hat{S}(t)$ and microorganism $\hat{X}(t)$ concentrations are shown in Figure 5. It can be noted that $\hat{S}(t)$ converges to its true value $S(t)$ with a rate specified by the dilution rate D only when the true inlet substrate concentration is exactly equal to its nominal value of S_{in}=50 g/L. Otherwise, the estimates $\hat{S}(t)$ can be highly inaccurate. In turn, the estimates $\hat{X}(t)$ do not converge to their true values $X(t)$ and this results from the lack of knowledge of the nonzero death rate k_d when designing the asymptotic observer. In spite of errors in the estimated substrate and microorganism concentrations, the adaptive and offset-free NMPCs ensure very good control performance and zero offset, while the classical NMPC drives the fermentation process close to the desired setpoint concentrations.

Scenario 2

In this scenario it is assumed that all the kinetic parameters (μ_m, K_s, and K_i) are constant, but not known exactly (parameter uncertainty). This is quite frequent situation, when the model parameters can be identified based on the available measurement data, but their values are determined with an uncertainty. Thus, only nominal values of the model parameters are known (Table 1), but true kinetic parameters (μ_m, K_s, and K_i) may differ by ±30% with respect to their nominal values: μ_m(true)=1.01 1/h; K_s(true)=1.21 g/L; K_i(true)=5.06 g/L. Moreover, only the nominal value of the inlet substrate concentration S_{in}=50 g/L is known and used by the NMPCs, but the true S_{in} may vary in a step-wise manner between 40 and 60 g/L.

The results presented in Figure 6, show that the adaptive and offset-free NMPCs are robust to modeling errors and the setpoint ethanol concentration can be tracked very well with zero offset. The resulting *ISE* indicators are: $ISE_{adapt.}$=941.1 (adaptive NMPC) and $ISE_{of.}$=940.0 (offset-free NMPC). In turn, the effectiveness of the classical NMPC is worse than in the Scenario 1 as the steady-state error has larger values and the performance indicator is $ISE_{class.}$=1145.5. In this scenario, all the NMPCs are also able to stabilize the fermentation process and eliminate the oscillatory behavior.

Scenario 3

Many experimental studies have shown that the specific growth rate μ not only depends on the substrate or product concentrations, but can also vary over time due to changes in temperature, pH, or the physiological state of microorganisms [38–40]. Therefore, in this scenario, it is additionally assumed that true kinetic parameters vary in time, but no more than ±30% with respect to its

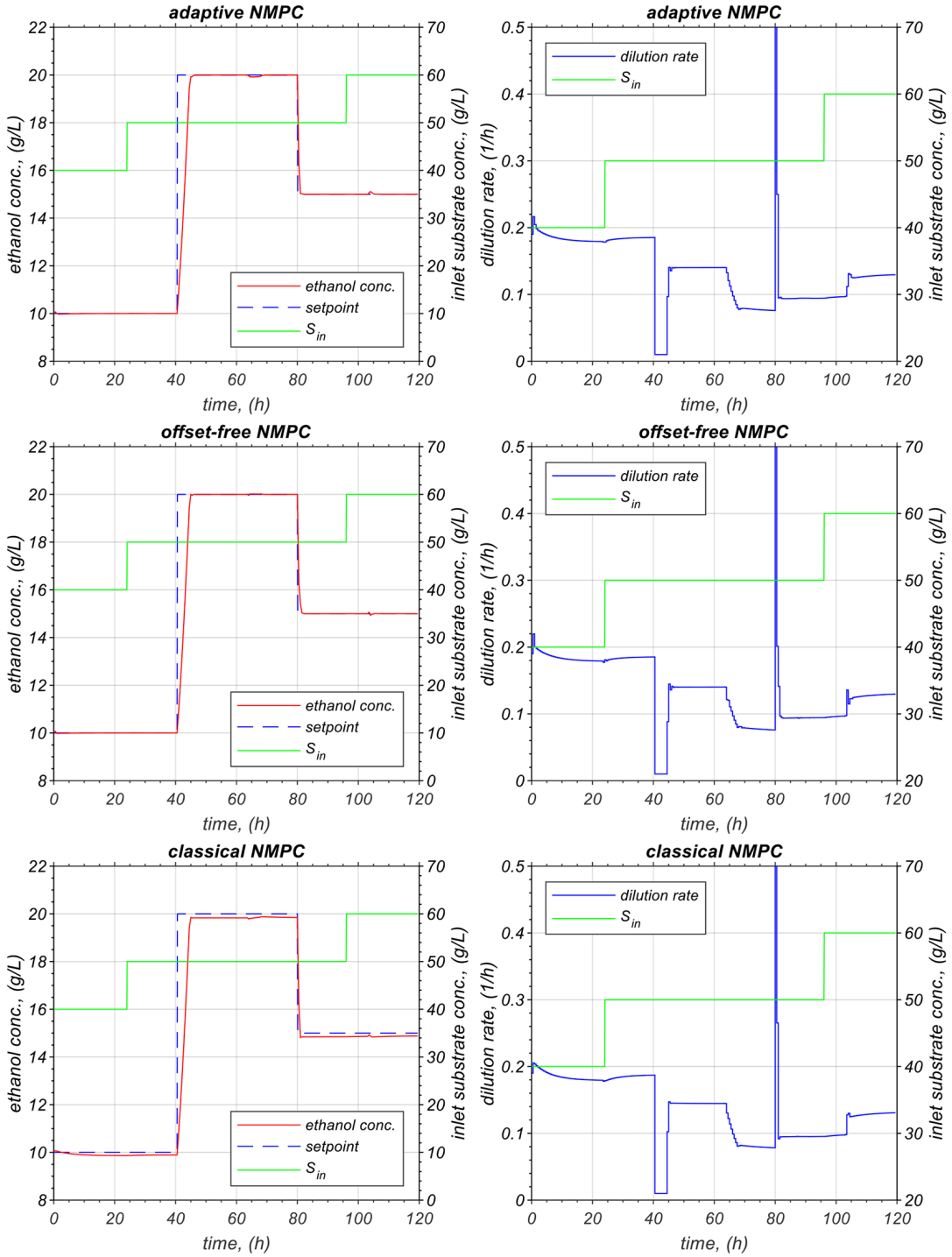

Figure 4. Time courses of ethanol concentration and corresponding dilution rate computed by three different NMPC algorithms (Scenario 1: variation in the unmeasured S_{in}; all other model parameters are constant and known)

nominal values, which poses an extra challenge for the predictive controllers:

$$\mu_m(t) = \mu_{m0} + 0.234\sin(0.025t - 0.5) \quad (47)$$

$$K_s(t) = K_{s0} + 0.519\sin(0.017t + 0.5) \quad (48)$$

$$K_i(t) = K_{i0} + 1.167\sin(0.031t - 3.1) \quad (49)$$

where: μ_{m0}=0.78 1/h, K_{s0}=1.73 g/L, and K_{i0}=3.89 g/L are known nominal values of kinetic parameters.

Moreover, it is assumed that the measured ethanol concentration is corrupted by noise. Thus, a Gaussian white noise of mean zero and standard deviation of σ=0.05 g/L is added to the measured

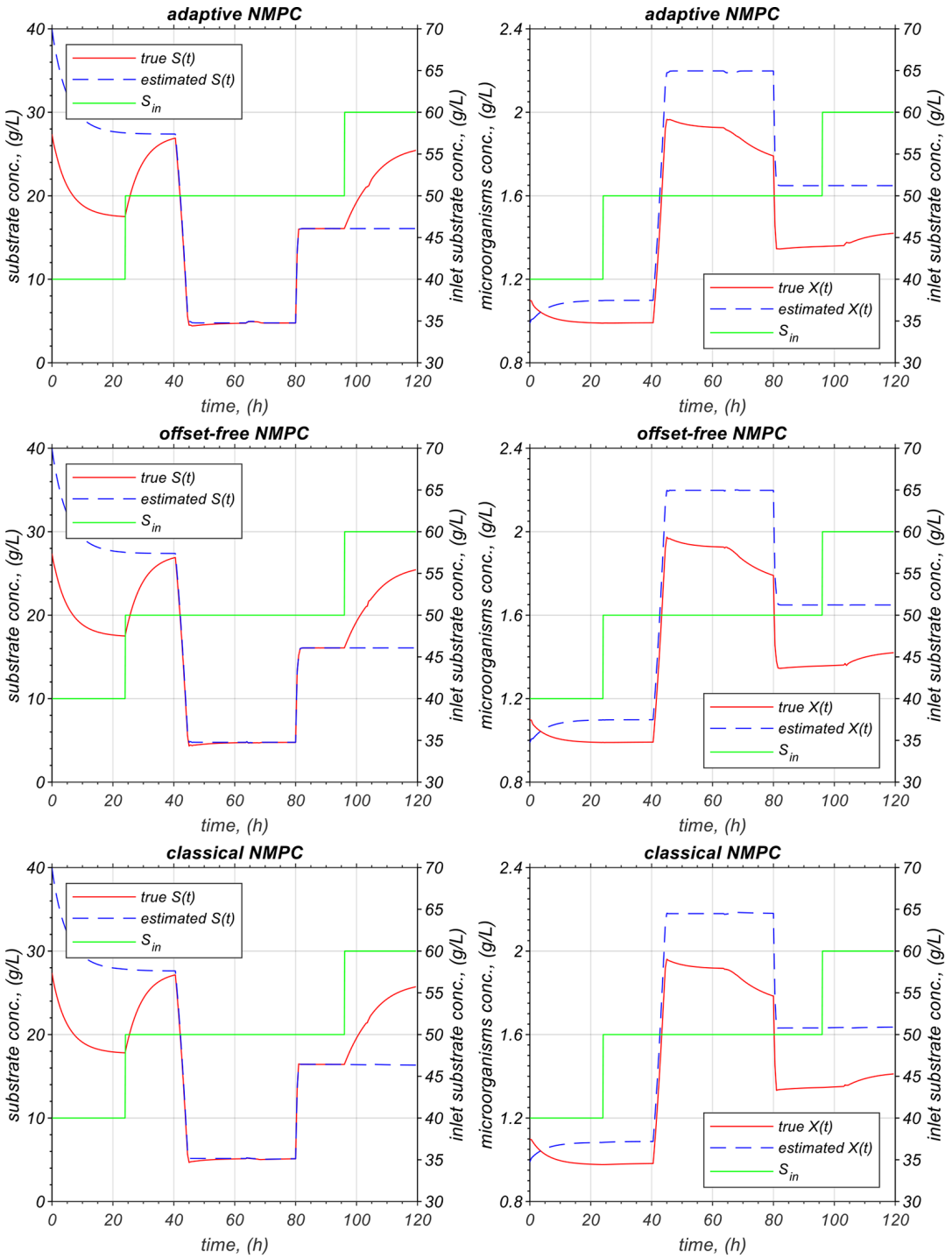

Figure 5. True and estimated substrate and microorganisms concentrations (Scenario 1: variation in the unmeasured S_{in}; all other model parameters are constant and known)

ethanol concentration P. This noise level is typical when measuring ethanol concentration online [29]. In order to compare all the NMPCs, in each simulation experiment the random numbers are generated using the same seed.

In this most challenging scenario, the adaptive and offset-free NMPCs again provided very good setpoint tracking. In the case of the adaptive NMPC, estimation of the maximum specific growth rate μ_m compensates for changes in other kinetic parameters. In turn, the classical NMPC is able to track the setpoint, but with small offset. Significant differences can be noticed when studying time courses of the manipulated variable (dilution rate D), which is manifested by its strong variations, especially

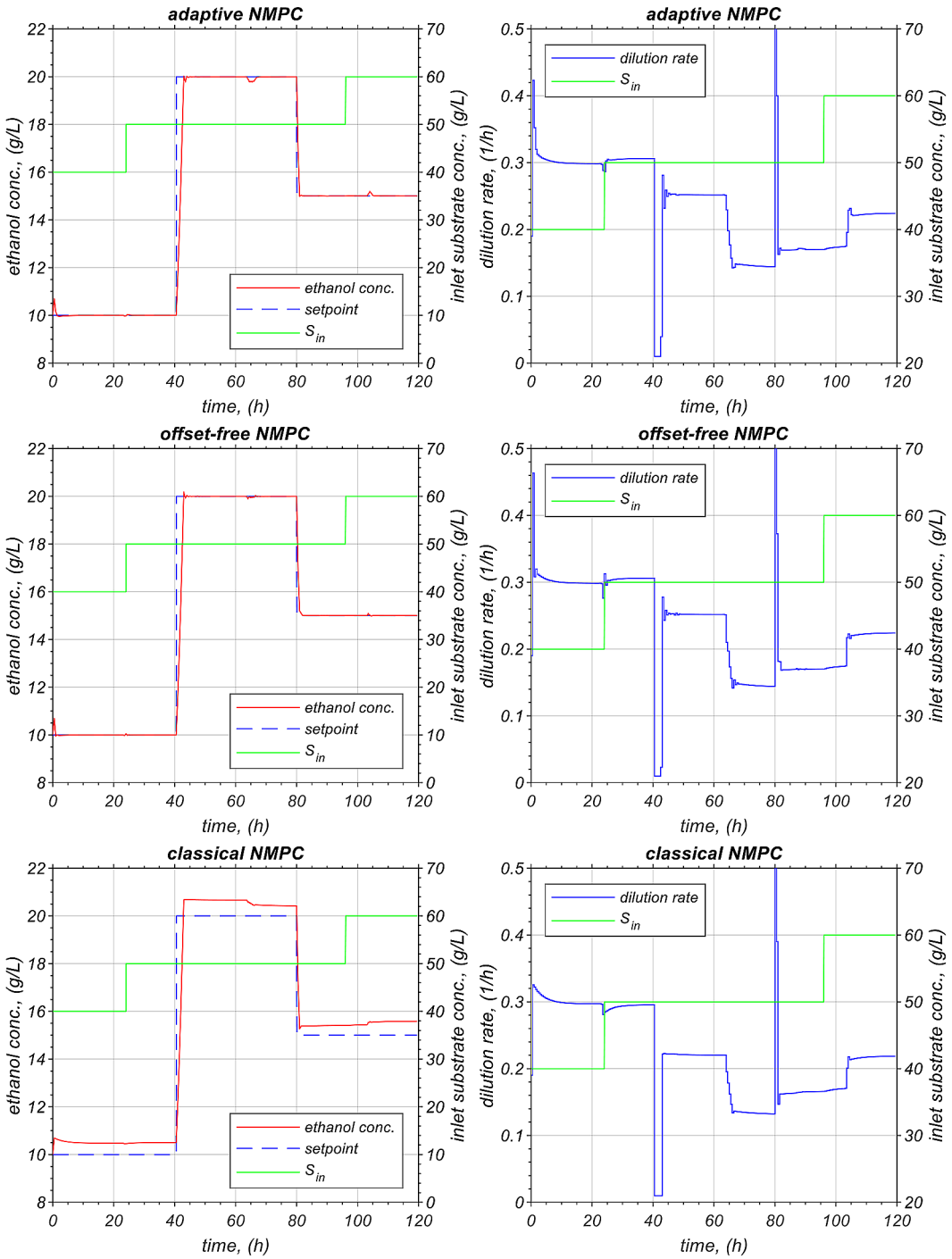

Figure 6. Time courses of ethanol concentration and corresponding dilution rate computed by three different NMPC algorithms (Scenario 2: variation in the unmeasured S_{in}; true kinetic parameters are unknown but constant)

for the offset-free NMPC. This is also reflected in the standard deviation σ_u of the manipulated variable calculated over the first 40 hours of the simulation (Table 2). A reason for the noise amplification probably lies in the offset-free mechanism. A correction term v, which is added to the discretized state-space Equation 43, is computed based on the noisy measurements. In the adaptive NMPC, the noisy measurements are additionally filtered by the observer Equations 37–39. It is expected that after adding noise filtering to the offset-free NMPC, the effect of the amplified noise can be reduced.

The average computation times in each controller sampling period were: 71 ms (but no more than 350 ms) for the adaptive NMPC, 121 ms (but

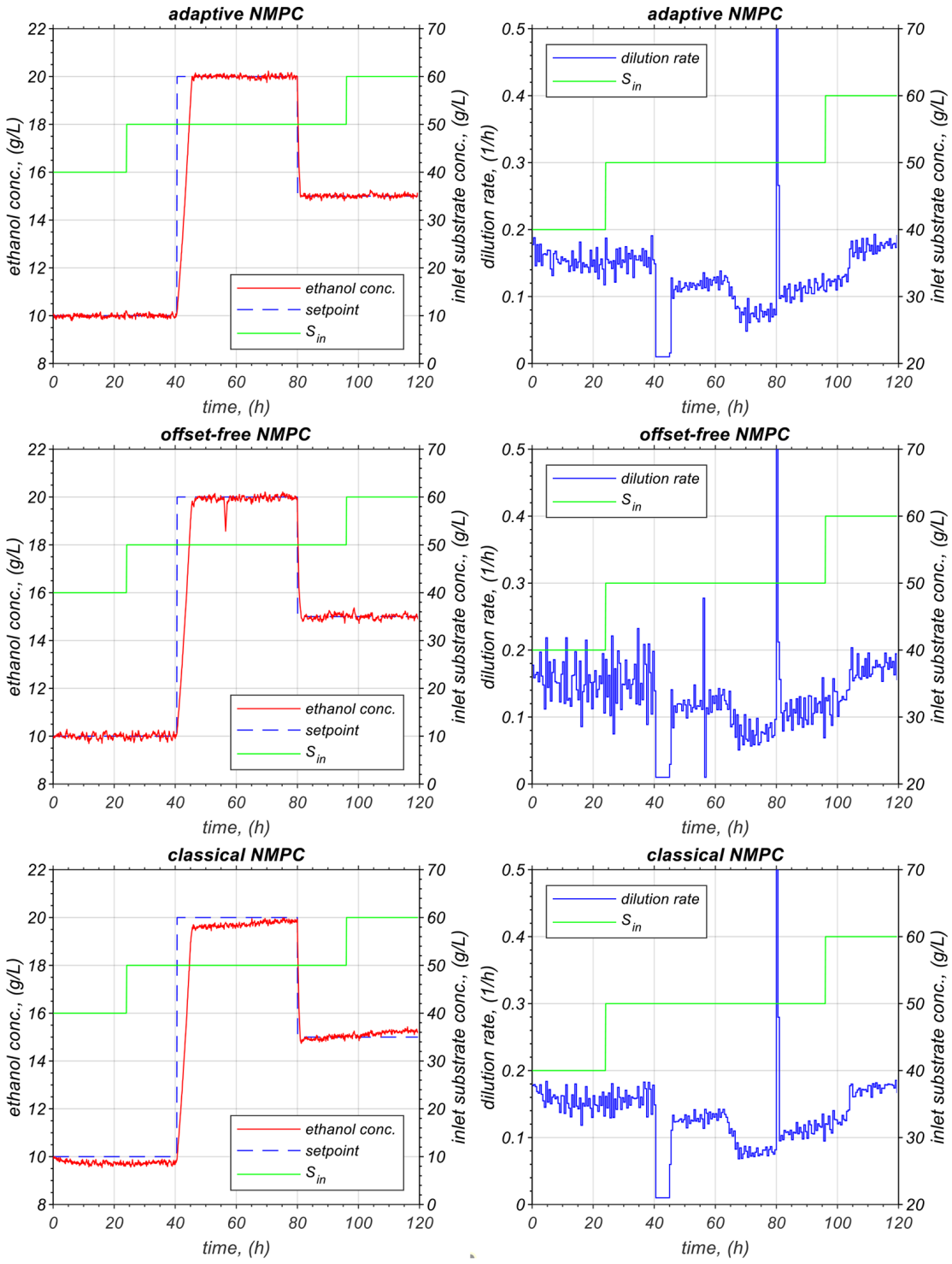

Figure 7. Time courses of ethanol concentration and corresponding dilution rate computed by three different NMPC algorithms (Scenario 3: variation in the unmeasured S_{in}; true kinetic parameters are unknown vary in time)

no more than 500 ms) for the offset-free NMPC, and 62 milliseconds (but no more than 350 ms) for the classical NMPC. As the controller sampling time was set to T_s=0.5 h, the computation time poses no implementation problems.

Finally, all performance indicators calculated for each scenario and each control algorithm are presented in Table 2 and the smallest values of *ISE* indicators are bolded.

Table 2. Performance indicators obtained for NMPCs

Algorithm	Scen. 1	Scen. 2	Scen. 3	
	ISE	*ISE*	*ISE*	σ_u
Adaptive NMPC	**1579.6**	941.1	**1842.9**	**0.0150**
Offset-free NMPC	1580.6	**940.0**	1851.2	0.0337
Classical NMPC	1639.1	1145.5	2011.2	0.0152

CONCLUSIONS

The stability analysis of the open-loop fermentation process revealed that the delayed ethanol inhibitory effect is responsible for the oscillatory behavior in the process. Based on the derived stability conditions, it was possible to study the effects of dilution rates and kinetic parameters on the dynamical behavior of the open-loop fermentation process and the steady-state ethanol concentrations.

Then, the nonlinear model predictive controllers (NMPCs) were designed to stabilize the process. Although the unmeasured substrate and microorganism concentrations were not estimated accurately, the proposed adaptive NMPC ensured very good setpoint tracking with zero offset in a wide range of operating conditions. Treating the specific growth rate μ as a model parameter and estimating it online can compensate for the effects of other unknown kinetic parameters, unmeasured variations in the inlet substrate concentration S_{in}, or structural discrepancies in the model. Compared to other NMPC algorithms, the adaptive NMPC was less sensitive to the measurement noise. In terms of the *ISE* indicators, the control performance of the adaptive and offset-free NMPCs was nearly the same in Scenarios 1 and 2, whereas the indicators obtained for the classical NMPC were up to 20% higher. In Scenario 3, i.e., in the presence of measurement noise and time varying kinetic parameters, the smallest value of the *ISE* indicator was obtained for the adaptive NMPC (*ISE*=1842.9), while the *ISE* indicators for the offset-free and classical NMPCs were higher by 0.45% and 9.13%, respectively. Moreover, the effect of measurement noise on the manipulated variable was smallest for the adaptive and classical NMPCs (the standard deviation $\sigma_u \approx 0.015$) and approximately twice as high in the case of offset-free NMPC ($\sigma_u \approx 0.034$). Also, the average computation time was shortest for the adaptive NMPC (71 ms) and the classical NMPC (62 ms) and approximately twice as long for the offset-free NMPC (121 ms).

The predictive controllers were tested for the fermentation process with relatively low inlet substrate concentrations (S_{in}<100 g/L). This raises the question of how the dynamical behavior of the open-loop process would change in a very high-gravity fermentation process, where inlet concentrations can reach up to 300 g/L. In that case the mathematical model (1–4) must include the additional effect of substrate inhibition, which would result in multiplicity of steady-states. The problem would become even more complex if model (1–4) also included the delayed effect of ethanol concentration. This would, of course, pose an additional challenge for controller design that aims at maximizing the bioreactor's productivity.

Acknowledgments

This work was supported by the grant from Silesian University of Technology – subsidy for maintaining and developing research potential in 2026.

REFERENCES

1. Jain S., Kumar S. A comprehensive review of bioethanol production from diverse feedstocks: Current advancements and economic perspectives. Energy. 2024; 296: 131130. https://doi.org/10.1016/j.energy.2024.131130
2. Chai W.Y., Teo K.T., Tan M.K., Tham H.J. Fermentation process control and optimization. Chem. Eng. Technol. 2022; 45(10): 1731–47. https://doi.org/10.1002/ceat.202200029
3. Bai F.W., Chen L.J., Anderson W.A., Moo-Young M. Parameter oscillations in a very high gravity medium continuous ethanol fermentation and their attenuation on a multistage packed column bioreactor system. Biotechnol. Bioeng. 2004; 88(5): 558–66. https://doi.org/10.1002/bit.20221
4. Bai F.W., Anderson W.A., Moo-Young M. Ethanol fermentation technologies from sugar and starch feedstocks. Biotechnol. Adv. 2008; 26(1): 89–105. https://doi.org/10.1016/j.biotechadv.2007.09.002

5. Li C.C. Mathematical models of ethanol inhibition effects during alcohol fermentation. Nonlinear Anal., Theory Methods Appl. 2009; 71(12): e1608–19. https://doi.org/10.1016/j.na.2009.02.004
6. Skupin P., Metzger M. Stability analysis of the continuous ethanol fermentation process with a delayed product inhibition. Appl. Math. Model. 2017; 49: 48–58. https://doi.org/10.1016/j.apm.2017.04.025
7. Astudillo I.C., Alzate C.A. Importance of stability study of continuous systems for ethanol production. J. Biotechnol. 2011; 151(1): 43–55. https://doi.org/10.1016/j.jbiotec.2010.10.073
8. Díaz-Quezada S., Wilson D.I., Pérez-Correa J.R. Modeling and simulation of a packed column batch still for fruit wine distillations. IEEE Access. 2022; 10: 84694–709. https://doi.org/10.1109/ACCESS.2022.3197604
9. Xinming C., Kaiqiang Z., Chi Z. Analyze and control on the membrane ethanol fermentation process with periodic exogenous signals. Chem. Eng. Process. Process Intensif. 2022; 181: 109174. https://doi.org/10.1016/j.cep.2022.109174
10. Watt S., Sidhu H., Nelson M., Ray A. Analysis of a model for ethanol production through continuous fermentation: Ethanol productivity. Int. J. Chem. React. Eng. 2010; 8(1): 1–17. https://doi.org/10.2202/1542-6580.1891
11. Skupin P., Metzger M. Oscillatory behaviour control in a continuous culture under double-substrate limitation. J. Biol. Dyn. 2018a; 12(1): 663–82. https://doi.org/10.1080/17513758.2018.1502368
12. Ciesielski A., Grzywacz R. Nonlinear analysis of cybernetic model for aerobic growth of Saccharomyces cerevisiae in a continuous stirred tank bioreactor. Static bifurcations. Biochem. Eng. J. 2019; 146: 88–96. https://doi.org/10.1016/j.bej.2019.03.003
13. Ciesielski A., Grzywacz R. Dynamic bifurcations in continuous process of bioethanol production under aerobic conditions using Saccharomyces cerevisiae. Biochem. Eng. J. 2020; 161: 107609. https://doi.org/10.1016/j.bej.2020.107609
14. Mustafa I.H. Two-parameter continuation and bifurcation strategies for oscillatory behavior elimination from a *Zymomonas mobilis* fermentation system. Chem. Eng. Technol. 2015; 38(8): 1362–70. https://doi.org/10.1109/37.1873
15. Toro J.C., Dobrosz-Gómez I., Gómez-García M.Á., Prat J., Massana I. A structured study on the dynamic bifurcation behavior of a continuous ethanol fermentor. Chem. Eng. Sci. 2021; 243: 116777. https://doi.org/10.1016/j.ces.2021.116777
16. Zhai C., Sun W., Palazoglu A. Analysis of periodically forced bioreactors using nonlinear transfer functions. J. Proc. Control. 2017; 58: 90–105. https://doi.org/10.1016/j.jprocont.2017.08.016
17. Alvarez-Ramirez J., Alvarez J. PI regulation for a class of bioreactors: stability and performance. Int. J. Robust Nonlinear Control. 2014; 24(5): 918–29. https://doi.org/10.1002/rnc.2926
18. Skupin P., Metzger M. PI control for a continuous fermentation process with a delayed product inhibition. J. Proc. Control. 2018b; 72: 30–8. https://doi.org/10.1016/j.jprocont.2018.09.011
19. Veselý V., Ilka A. Gain-scheduled PID controller design. J. Proc. Control. 2013; 23(8): 1141–8. https://doi.org/10.1016/j.jprocont.2013.07.002
20. Ajbar A., Ali E. Study of advanced control of ethanol production through continuous fermentation. J. King Saud Univ. Eng. Sci. 2017; 29(1): 1–11. https://doi.org/10.1016/j.jksues.2015.10.005
21. Mohd N., Aziz N. Control of bioethanol fermentation process: NARX-based MPC (NARX-MPC) versus linear-based MPC (LMPC). Chem. Eng. Trans. 2015; 45: 1297–302. https://doi.org/10.3303/CET1545217
22. Tatjewski P., Ławryńczuk M. Algorithms with state estimation in linear and nonlinear model predictive control. Comput. Chem. Eng. 2020; 143: 107065. https://doi.org/10.1016/j.compchemeng.2020.107065
23. Skupin P., Łaszczyk P., Goud E.C., Vooradi R., Ambati S.R. Robust nonlinear model predictive control of cascade of fermenters with recycle for efficient bioethanol production. Comput. Chem. Eng. 2022; 160: 107735. https://doi.org/10.1016/j.compchemeng.2022.107735
24. Bannoud M.A., Ferreira P.H., de Andrade R.R., da Silva C.A. Control of an integrated first and second-generation continuous alcoholic fermentation process with cell recycling using model predictive control. Chem. Eng. Commun. 2025; 212(4): 521–44. https://doi.org/10.1080/00986445.2024.2417901
25. Bakošová M., Oravec J., Vasičkaninová A., Mészáros A., Artzová P. Advanced Control of a Biochemical Reactor for Yeast Fermentation. Chem. Eng. Trans. 2019; 769–74. https://doi.org/10.3303/CET1976129
26. Montague G.A., Morris A.J., Bush J.R. Considerations in control scheme development for fermentation process control. IEEE Contr. Syst. Mag. 2002; 8(2): 44–8. https://doi.org/10.1109/37.1873
27. Ruan S., Wei J. On the zeros of transcendental functions with applications to stability of delay differential equations with two delays. Dyn. Contin. Discrete Impuls. Syst. A: Math. Anal. 2003; 10(6): 863–74.
28. Feng Y., Tian X., Chen Y., Wang Z., Xia J., Qian J., Zhuang Y., Chu J. Real-time and on-line monitoring of ethanol fermentation process by viable cell sensor and electronic nose. Bioresour. Bioproc. 2021; 8(1): 37. https://doi.org/10.1186/s40643-021-00391-5

29. Renard F., Vande Wouwer A. Robust adaptive control of yeast fed-batch cultures. Comput. Chem. Eng. 2008; 32(6): 1238–48. https://doi.org/10.1016/j.compchemeng.2007.05.008
30. Bastin G., Dochain D. On-line estimation and adaptive control of bioreactors. Elsevier; 1990. https://doi.org/10.1016/C2009-0-12088-3
31. Dochain D. State and parameter estimation in chemical and biochemical processes: a tutorial. J. Proc. Control. 2003; 13(8): 801–18. https://doi.org/10.1016/S0959-1524(03)00026-X
32. De Battista H., Picó J., Garelli F., Vignoni A. Specific growth rate estimation in (fed-) batch bioreactors using second-order sliding observers. J. Proc. Control. 2011; 21(7): 1049–55. https://doi.org/10.1016/j.jprocont.2011.05.008
33. Jamilis M., Garelli F., Mozumder M.S., Volcke E., De Battista H. Specific growth rate observer for the growing phase of a polyhydroxybutyrate production process. Bioprocess Biosyst. Eng. 2015; 38(3): 557–67. https://doi.org/10.1007/s00449-014-1295-1
34. Claes J.E., Van Impe J.F. On-line estimation of the specific growth rate based on viable biomass measurements: experimental validation. Bioprocess Eng. 1999; 21(5): 389–95. https://doi.org/10.1007/s004490050692
35. Ławryńczuk M., Tatjewski P. Offset-free state-space nonlinear predictive control for Wiener systems. Inf. Sci. 2020; 511: 127–51. https://doi.org/10.1016/j.ins.2019.09.042
36. Wächter A., Biegler L.T. On the implementation of an interior-point filter line-search algorithm for large-scale nonlinear programming. Math. Program. 2006; 106(1): 25–57. https://doi.org/10.1007/s10107-004-0559-y
37. Allgower F, Findeisen R, Nagy ZK. Nonlinear model predictive control: From theory to application. J. Chin. Inst. Chem. Engrs. 2004; 35(3): 299–316. https://doi.org/10.6967/JCICE.200405.0299
38. Azhar S.H., Abdulla R., Jambo S.A., Marbawi H., Gansau J.A., Faik A.A., Rodrigues K.F. Yeasts in sustainable bioethanol production: A review. Biochem. Biophys. Rep. 2017; 10: 52–61. https://doi.org/10.1016/j.bbrep.2017.03.003
39. Lin Y., Zhang W., Li C., Sakakibara K., Tanaka S., Kong H. Factors affecting ethanol fermentation using *Saccharomyces cerevisiae* BY4742. Biomass Bioenergy. 2012; 47: 395–401. https://doi.org/10.1016/j.biombioe.2012.09.019
40. Salakkam A., Phukoetphim N., Laopaiboon P., Laopaiboon L. Mathematical modeling of bioethanol production from sweet sorghum juice under high gravity fermentation: Applicability of Monod-based, logistic, modified Gompertz and Weibull models. Electron. J. Biotechnol. 2023; 64: 18–26. https://doi.org/10.1016/j.ejbt.2023.03.004